



Indian Institute of Information Technology Vadodara - International Campus Diu
Institute of National Importance declared by an act of Parliament
Education Hub, Kevdi, Diu (U.T) - 362520

Comparative Analysis of Table Recognition.

This is the group project of course CS391

Mentored By-

Dr. Deepika Gupta

Submitted by

Group - 01

Group Members:

Ishaan Ashish Arora - 202011012

Yashesh Bhavsar - 202011017

Dev Juneja - 202011020

Hari Gopal Nayak Jarupla - 202011024

Suraj Kumar - 202011069

November 2022

Content

| | |
|---------------------------------|---|
| (1) Introduction | 3 |
| (2) Model1:YOLOv3 | 4 |
| (3) Model2:VGG-19 | 4 |
| (4) Model3:Faster-CNN | 6 |
| (5) Model4:RCNN-HRNet | 7 |
| (6) Experimental Analysis | 8 |
| (7) Conclusion | 8 |

Abstract

In this particular report, we discuss the comparative analysis of the table detection models that have been developed. In our analysis, we focused on the precision, accuracy and F1 scores of the respective models. Based on the findings we try to decide on an efficient model which provides better results. In the process, we analyze the shortcomings of each of the four models. We have provided the numerical analysis of all the models. Upon training and running all the models we analysed the functioning. The motivation behind this analysis was to come up with the best possible solution to the problem of table detection(recognition)

Keywords RCNN-HRNet,Faster-CNN(FRCNN),YOLOv3,VGG-19

1 Introduction

The world is evolving, becoming more digitalized. Digital documents are increasingly replacing paper-based ones. These papers include various table-based data with different appearances and layouts and alignments. Table identification and table structure recognition are two subtasks of an automated table information extraction approach. While table structure recognition identifies the rows and columns to identify individual table cells, table detection identifies the area of the picture that contains the table. We have used RCNN/HRNet as an enhanced deep learning-based end-to-end method for resolving the two sub-problems with a single model. Instance segmentation is used to address the issue of table detection. Each image undergoes table segmentation, which aims to pinpoint every instance of the table at the pixel level inside the image. To determine the structure of the table, we similarly execute table cell segmentation on each picture to forecast segmented portions of table cells inside each table. The model simultaneously predicts table and cell areas in a single inference. The model simultaneously divides tables into two categories: bordered (based on rules) and borderless (without rules).

For extracting cells from bordered tables, we use rule-based conventional text detection and line detection algorithms. We show how iterative transfer learning works to help CNN learn from less training data while also enabling it to excel on various datasets by fine-tuning it on the appropriate datasets. A novel approach of image augmentation was also inserted into the training process to enhance the accuracy of table identification and enable it learn efficiently. In order to comprehend tabular data in document pictures, an automatic table identification approach must first solve the challenges of table detection

and table structure recognition. Deep learning-based solutions are being used in more recent efforts, which also try to create an end-to-end solution. The Convolution Neural Network (CNN) model, provides an enhanced deep learning-based end-to-end method in this research for handling the issues of table identification and structure recognition. The models have tested on publicly available datasets from ICDAR 2013, ICDAR 2019, and Table-Bank. We test the accuracy results for the ICDAR 2013 and Table-Bank dataset. Additionally, using the ICDAR 2019 table structure identification dataset.

CHAPTER 2 • PROGRESS IN ONLINE SERVICE DELIVERY

Table 2.6. High online service performance relative to income

| Country | Online Service Index | Income group |
|------------|----------------------|--------------|
| Rwanda | 0.5118 | Low |
| Colombia | 0.7874 | Upper Middle |
| Ethiopia | 0.4567 | Low |
| Kazakhstan | 0.7480 | Upper Middle |
| Morocco | 0.6929 | Lower Middle |
| Kenya | 0.4252 | Low |
| Sri Lanka | 0.6335 | Lower Middle |
| Malaysia | 0.6772 | Upper Middle |
| Tunisia | 0.6378 | Upper Middle |
| Mongolia | 0.6142 | Lower Middle |

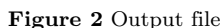
Table 2.7. Low online service performance relative to income

| Country | Online Service Index | Income group |
|-----------------------|----------------------|--------------|
| Equatorial Guinea | 0.0315 | High |
| Monaco | 0.2205 | High |
| Libya | 0.0157 | Upper Middle |
| Saint Kitts and Nevis | 0.1339 | High |
| San Marino | 0.2756 | High |
| Tuvalu | 0.0394 | Upper Middle |
| Barbados | 0.2205 | High |
| Algeria | 0.0787 | Upper Middle |
| Sao Tome and Principe | 0.0079 | Lower Middle |

Ultimately, the measure of online service utility is its impact on development either directly in provision of services to citizens or indirectly, for example through investment linked to apparent ease of doing business. Low- and middle-income countries with relatively low levels of Internet use such as Ethiopia (1.48 per cent of the population are Internet users), Rwanda (8.02 per cent of the population are Internet users) and Sri Lanka (18.29 per cent of the population are Internet users), and relatively high online service scores may need to invest more in securing telecommunication infrastructure to fully optimize the benefit of e-services.

The converse also applies to high income countries with widespread telecommunication infrastructure and low online service scores such as Monaco (87.00 per cent of the population are Internet users), Saint Kitts and Nevis (79.35 per cent of the population are Internet users) and Barbados (73.33 per cent of the population are Internet users). These are all small countries, and it may be the case that a larger critical mass of Internet users, or potential users, makes it more worthwhile for a country to invest in resource intensive forms of online service delivery such as remote health care, smart energy grids and real-time environmental monitoring. The Survey does not, however, require such technological advancement for high scores reflecting the view that even relatively simple information sharing and interaction can produce important benefits when the primary needs and attributes of population segments are reflected in online service design.

Figure 1 Input file



In this model, a YOLO-based method is used. Considering the large difference between document objects and natural objects, this architecture introduces some adaptive adjustments to YOLOv3, including an anchor optimization strategy and two post-processing methods. For anchor optimization, the model uses k-means clustering to find anchors which are more suitable for tables rather than natural objects and make it easier for our model to find the exact positions of tables. In the post-processing process, the extra whitespaces and noisy page objects (e.g. page headers, page footers and other similar objects) are removed from the predicted results so that the model can get more accurate table margins and higher IoU scores. The model is evaluated on two datasets from ICDAR 2013 and ICDAR 2017 and achieves state-of-the-art performance.

Algorithm 1: Erasing whitespace margin algorithm

```

1 orientations = {up, down, left, right};
2 R = P;
3 for ori in orientations do
4     M = {all pixels belong to the margin of R in
        direction ori};
5     while all pixels  $\in$  M are white color do
6         R = R - M;
7         M = {all pixels belong to the margin of R in
            direction ori};
8     end
9 end
10 return R;

```

2.2 Dataset performance

2.3 Conclusion from the model

3 Model2:VGG-19

3.1 Algorithm

The model uses a pre-trained VGG-19 layer as the base network. The fully connected layers (layers after pool5) of VGG-19 are replaced with two (1x1) convolution layers. Each of these convolution layers (conv6) uses the ReLU activation followed by a dropout layer having probability of 0.8 (conv6 + dropout). Following this layer, two different branches of the decoder network are appended. This is according to the intuition that the column region is a subset of the table

region. Thus, the single encoding network can filter out the active regions with better accuracy using features of both table and column regions. The output of the (conv6 + dropout) layer is distributed to both decoder branches. In each branch, additional layers are appended to filter out the respective active regions. In the table branch of the decoder network, an additional (1x1) convolution layer, conv7 table is used, before using a series of fractionally strided convolution layers for upscaling the image. The output of the conv7 table layer is also up-scaled using fractionally strided convolutions, and is appended with the pool4 pooling layer of the same dimension. Similarly, the combined feature map is again up-scaled and the pool3 pooling is appended to it. Finally, the final feature map is up-scaled to meet the original image dimension.

3.2 Dataset performance

VGG-19 requires both table and structure annotated data for training. The Marmot table detection dataset and manually annotated the structure information were used. There are a total of 1016 documents containing tables including both Chinese and English documents, out of which 509 English documents are annotated and used for training. In this model we get the recall as 0.9501, precision as 0.9547 and F1-score as 0.9547.

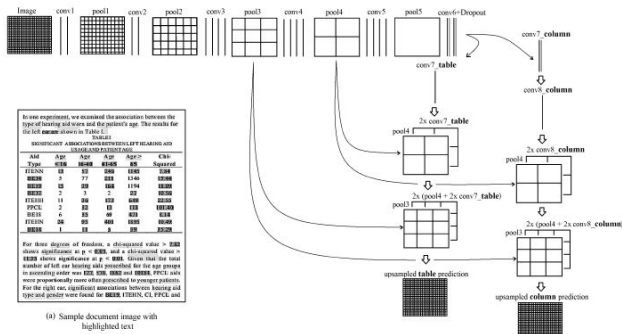


Figure 4 VGG-19

Table 1. Actual and projected numbers for enrollment in grades PK-12, PK-6, and 9-12 in elementary and secondary schools, by control of school: Fall 1996 through Fall 2021 (in thousands)

| Year | Total | | | Public | | | Private | | |
|-----------|--------|--------|--------|--------|--------|--------|---------|-------|-------|
| | PK-12 | PK-6 | 9-12 | PK-12 | PK-6 | 9-12 | PK-12 | PK-6 | 9-12 |
| Actual | | | | | | | | | |
| 1996 | 51,544 | 37,481 | 14,063 | 45,611 | 32,782 | 12,829 | 5,933 | 4,719 | 1,213 |
| 1997 | 52,071 | 37,797 | 14,275 | 46,127 | 33,071 | 13,056 | 5,944 | 4,729 | 1,219 |
| 1998 | 52,226 | 38,091 | 14,135 | 46,339 | 33,341 | 13,192 | 5,988 | 4,747 | 1,240 |
| 1999 | 52,375 | 38,251 | 14,125 | 46,537 | 33,485 | 13,371 | 6,018 | 4,764 | 1,254 |
| 2000 | 52,375 | 38,254 | 14,125 | 46,537 | 33,485 | 13,371 | 6,018 | 4,767 | 1,252 |
| 2001 | 52,392 | 38,269 | 14,125 | 46,572 | 33,485 | 13,371 | 6,020 | 4,763 | 1,257 |
| 2002 | 54,403 | 39,000 | 15,403 | 48,183 | 34,114 | 14,069 | 6,220 | 4,883 | 1,335 |
| 2003 | 54,526 | 39,262 | 15,264 | 48,540 | 34,301 | 14,239 | 6,209 | 4,761 | 1,338 |
| 2004 | 54,582 | 39,308 | 15,274 | 48,735 | 34,178 | 14,518 | 6,197 | 4,731 | 1,399 |
| 2005 | 55,187 | 39,363 | 15,823 | 49,113 | 34,201 | 14,909 | 6,173 | 4,689 | 1,371 |
| 2006 | 55,307 | 39,338 | 16,480 | 49,318 | 34,239 | 15,081 | 6,191 | 4,604 | 1,388 |
| 2007 | 55,653 | 39,722 | 16,481 | 49,233 | 34,203 | 15,037 | 6,210 | 4,517 | 1,384 |
| 2008 | 54,973 | 38,620 | 16,353 | 48,265 | 34,268 | 14,990 | 5,707 | 4,335 | 1,373 |
| 2009 | 51,882 | 38,560 | 16,793 | 46,373 | 34,118 | 14,055 | 5,188 | 4,181 | 1,338 |
| 2010 | 54,376 | 38,716 | 16,180 | 48,483 | 34,675 | 14,808 | 5,391 | 4,691 | 1,300 |
| Projected | | | | | | | | | |
| 2011 | 54,366 | 38,699 | 16,247 | 48,438 | 34,849 | 14,787 | 5,320 | 4,660 | 1,260 |
| 2012 | 55,291 | 39,115 | 15,876 | 49,826 | 35,073 | 14,752 | 5,253 | 4,639 | 1,234 |
| 2013 | 55,286 | 39,334 | 15,954 | 50,067 | 35,301 | 14,756 | 5,221 | 4,633 | 1,188 |
| 2014 | 55,559 | 39,239 | 16,260 | 50,407 | 35,562 | 14,805 | 5,192 | 4,637 | 1,155 |
| 2015 | 55,357 | 39,780 | 16,189 | 50,773 | 35,735 | 15,038 | 5,163 | 4,653 | 1,130 |
| 2016 | 56,330 | 40,114 | 16,217 | 51,183 | 36,029 | 15,118 | 5,165 | 4,665 | 1,100 |
| 2017 | 56,722 | 40,451 | 16,271 | 51,624 | 36,339 | 15,195 | 5,188 | 4,722 | 1,076 |
| 2018 | 57,066 | 40,797 | 16,301 | 51,880 | 36,639 | 15,241 | 5,218 | 4,768 | 1,061 |
| 2019 | 57,367 | 41,149 | 16,338 | 52,080 | 36,869 | 15,294 | 5,247 | 4,783 | 1,054 |
| 2020 | 57,375 | 41,506 | 16,486 | 52,088 | 37,278 | 15,410 | 5,267 | 4,795 | 1,059 |
| 2021 | 58,144 | 41,981 | 16,583 | 53,113 | 37,698 | 15,515 | 5,351 | 4,863 | 1,080 |

Figure 5 VGG-19: raw input image

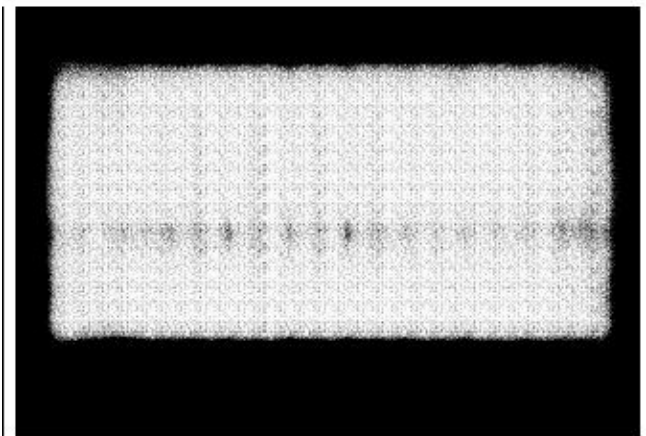


Figure 6 VGG-19 table mask

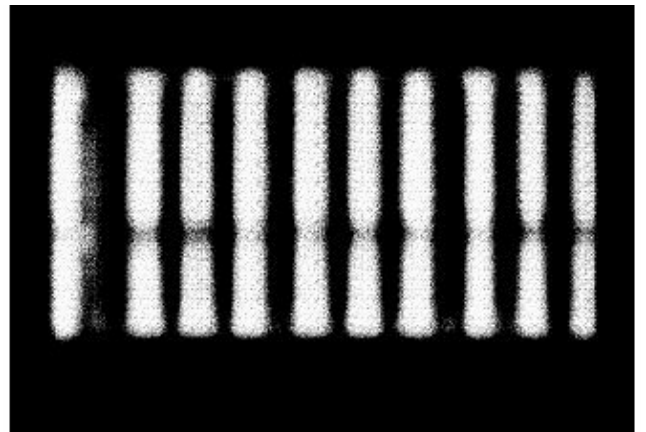


Figure 7 VGG-19 column mask

3.3 Conclusion from the model

The VGG-19 model is a novel deep learning model trained on dual tasks of table detection and structure recognition in an end-to-end fashion. Existing approaches to information extraction treat detection

and structure recognition as two distinct problems to be solved independently. VGG-19 is the first model to jointly address both tasks simultaneously, by exploiting the inherent interdependence between table detection and table structure identification. VGG-19 utilizes the knowledge from previously learned tasks and can transfer that knowledge to newer, related ones demonstrating transfer learning.

4 Model3:Faster-CNN

This model is an end-to-end system for table detection and structure recognition in document images called FCNN. This method is data driven, based on deep learning, and hence does not require any heuristics or rules to detect tables and to recognize their structure. This approach makes FCNN applicable to both, images as well as born-digital documents (e.g. PDFs, Word documents, and web pages, as they can be converted to images).

4.1 Algorithm

The first step in table understanding is detecting the locations of tables within a document. Conceptually, the problem is similar to the detection of objects in natural scene images. Therefore, in this approach domain adaptation is used and transfer learning by utilizing deep learning-based object detection frameworks originally created for natural scene images and tested their ability to cope with tabular structures in scanned document images.

The FRCNN model consists of two distinct parts: First they generate region proposals based on the input image by a so-called region proposal network (RPN). Afterwards, these proposals are classified using a Fast-RCNN network. Both modules share parameters and can be trained end-to-end.

After a table has successfully been detected and its location is known to the system, the next step is in understanding its contents to recognize and locate the rows and columns which make up the physical structure of the table. This step is inherently different from the preceding table detection. The key difference is not only that there are significantly more rows and columns present in a table image than there are tables in a document but these tabular structures are generally located in very close proximity. These two factors make this task so difficult for FRCNN and ask for a different approach.

4.2 Dataset performance

As FCNN is based on a data-driven approach, there was the need for a sufficiently large dataset. The largest the publicly available dataset is the Marmot dataset for table recognition¹ published by the Insti-

tute of Computer Science and Technology of Peking University.

The FCN-based segmentation models of FCNN were trained for 60,000 iterations employing a standard SGD optimizer with a fixed learning rate of 10-10 and classical the momentum of 0.99.

by education system: 2011

| Education system | Percentage of population | National average | Weighted school participation rate | Weighted school participation rate after substitution | Weighted school participation rate | Combined weighted school participation and student response rate |
|----------------------|--------------------------|------------------|------------------------------------|---|------------------------------------|--|
| Albania | 100 | 1 | 100 | 100 | 100 | 100 |
| Algeria | 100 | 1 | 100 | 100 | 100 | 100 |
| Angola | 100 | 1 | 100 | 100 | 100 | 100 |
| Argentina | 100 | 1 | 100 | 100 | 100 | 100 |
| Australia | 100 | 1 | 100 | 100 | 100 | 100 |
| Austria | 100 | 1 | 100 | 100 | 100 | 100 |
| Bahrain | 100 | 1 | 100 | 100 | 100 | 100 |
| Belgium | 100 | 1 | 100 | 100 | 100 | 100 |
| Brazil | 100 | 1 | 100 | 100 | 100 | 100 |
| Bulgaria | 100 | 1 | 100 | 100 | 100 | 100 |
| Canada | 100 | 1 | 100 | 100 | 100 | 100 |
| Chad | 100 | 1 | 100 | 100 | 100 | 100 |
| China | 100 | 1 | 100 | 100 | 100 | 100 |
| Colombia | 100 | 1 | 100 | 100 | 100 | 100 |
| Czech Republic | 100 | 1 | 100 | 100 | 100 | 100 |
| Denmark | 100 | 1 | 100 | 100 | 100 | 100 |
| Dominican Republic | 100 | 1 | 100 | 100 | 100 | 100 |
| Egypt | 100 | 1 | 100 | 100 | 100 | 100 |
| Finland | 100 | 1 | 100 | 100 | 100 | 100 |
| France | 100 | 1 | 100 | 100 | 100 | 100 |
| Germany | 100 | 1 | 100 | 100 | 100 | 100 |
| Ghana | 100 | 1 | 100 | 100 | 100 | 100 |
| Greece | 100 | 1 | 100 | 100 | 100 | 100 |
| Hong Kong | 100 | 1 | 100 | 100 | 100 | 100 |
| Hungary | 100 | 1 | 100 | 100 | 100 | 100 |
| India | 100 | 1 | 100 | 100 | 100 | 100 |
| Indonesia | 100 | 1 | 100 | 100 | 100 | 100 |
| Iran | 100 | 1 | 100 | 100 | 100 | 100 |
| Ireland | 100 | 1 | 100 | 100 | 100 | 100 |
| Israel | 100 | 1 | 100 | 100 | 100 | 100 |
| Italy | 100 | 1 | 100 | 100 | 100 | 100 |
| Japan | 100 | 1 | 100 | 100 | 100 | 100 |
| Kenya | 100 | 1 | 100 | 100 | 100 | 100 |
| Korea | 100 | 1 | 100 | 100 | 100 | 100 |
| Latvia | 100 | 1 | 100 | 100 | 100 | 100 |
| Lebanon | 100 | 1 | 100 | 100 | 100 | 100 |
| Lithuania | 100 | 1 | 100 | 100 | 100 | 100 |
| Malaysia | 100 | 1 | 100 | 100 | 100 | 100 |
| Mexico | 100 | 1 | 100 | 100 | 100 | 100 |
| Moldova | 100 | 1 | 100 | 100 | 100 | 100 |
| Morocco | 100 | 1 | 100 | 100 | 100 | 100 |
| Netherlands | 100 | 1 | 100 | 100 | 100 | 100 |
| New Zealand | 100 | 1 | 100 | 100 | 100 | 100 |
| Nigeria | 100 | 1 | 100 | 100 | 100 | 100 |
| North Macedonia | 100 | 1 | 100 | 100 | 100 | 100 |
| Poland | 100 | 1 | 100 | 100 | 100 | 100 |
| Portugal | 100 | 1 | 100 | 100 | 100 | 100 |
| Romania | 100 | 1 | 100 | 100 | 100 | 100 |
| Russia | 100 | 1 | 100 | 100 | 100 | 100 |
| Saudi Arabia | 100 | 1 | 100 | 100 | 100 | 100 |
| Slovakia | 100 | 1 | 100 | 100 | 100 | 100 |
| Slovenia | 100 | 1 | 100 | 100 | 100 | 100 |
| Spain | 100 | 1 | 100 | 100 | 100 | 100 |
| Sweden | 100 | 1 | 100 | 100 | 100 | 100 |
| Switzerland | 100 | 1 | 100 | 100 | 100 | 100 |
| Taiwan | 100 | 1 | 100 | 100 | 100 | 100 |
| Tanzania | 100 | 1 | 100 | 100 | 100 | 100 |
| Thailand | 100 | 1 | 100 | 100 | 100 | 100 |
| Togo | 100 | 1 | 100 | 100 | 100 | 100 |
| Turkey | 100 | 1 | 100 | 100 | 100 | 100 |
| Uganda | 100 | 1 | 100 | 100 | 100 | 100 |
| United Arab Emirates | 100 | 1 | 100 | 100 | 100 | 100 |
| United States | 100 | 1 | 100 | 100 | 100 | 100 |

Figure 8 FR-CNN output(row detecting)

by education system: 2011

| Education system | Percentage of population | National average | Weighted school participation rate | Weighted school participation rate after substitution | Weighted school participation rate | Combined weighted school participation and student response rate |
|----------------------|--------------------------|------------------|------------------------------------|---|------------------------------------|--|
| Albania | 100 | 1 | 100 | 100 | 100 | 100 |
| Algeria | 100 | 1 | 100 | 100 | 100 | 100 |
| Angola | 100 | 1 | 100 | 100 | 100 | 100 |
| Argentina | 100 | 1 | 100 | 100 | 100 | 100 |
| Australia | 100 | 1 | 100 | 100 | 100 | 100 |
| Austria | 100 | 1 | 100 | 100 | 100 | 100 |
| Bahrain | 100 | 1 | 100 | 100 | 100 | 100 |
| Belgium | 100 | 1 | 100 | 100 | 100 | 100 |
| Brazil | 100 | 1 | 100 | 100 | 100 | 100 |
| Bulgaria | 100 | 1 | 100 | 100 | 100 | 100 |
| Canada | 100 | 1 | 100 | 100 | 100 | 100 |
| Chad | 100 | 1 | 100 | 100 | 100 | 100 |
| China | 100 | 1 | 100 | 100 | 100 | 100 |
| Colombia | 100 | 1 | 100 | 100 | 100 | 100 |
| Czech Republic | 100 | 1 | 100 | 100 | 100 | 100 |
| Denmark | 100 | 1 | 100 | 100 | 100 | 100 |
| Dominican Republic | 100 | 1 | 100 | 100 | 100 | 100 |
| Egypt | 100 | 1 | 100 | 100 | 100 | 100 |
| Finland | 100 | 1 | 100 | 100 | 100 | 100 |
| France | 100 | 1 | 100 | 100 | 100 | 100 |
| Germany | 100 | 1 | 100 | 100 | 100 | 100 |
| Ghana | 100 | 1 | 100 | 100 | 100 | 100 |
| Greece | 100 | 1 | 100 | 100 | 100 | 100 |
| Hong Kong | 100 | 1 | 100 | 100 | 100 | 100 |
| Hungary | 100 | 1 | 100 | 100 | 100 | 100 |
| India | 100 | 1 | 100 | 100 | 100 | 100 |
| Indonesia | 100 | 1 | 100 | 100 | 100 | 100 |
| Iran | 100 | 1 | 100 | 100 | 100 | 100 |
| Ireland | 100 | 1 | 100 | 100 | 100 | 100 |
| Israel | 100 | 1 | 100 | 100 | 100 | 100 |
| Italy | 100 | 1 | 100 | 100 | 100 | 100 |
| Japan | 100 | 1 | 100 | 100 | 100 | 100 |
| Kenya | 100 | 1 | 100 | 100 | 100 | 100 |
| Korea | 100 | 1 | 100 | 100 | 100 | 100 |
| Latvia | 100 | 1 | 100 | 100 | 100 | 100 |
| Lebanon | 100 | 1 | 100 | 100 | 100 | 100 |
| Lithuania | 100 | 1 | 100 | 100 | 100 | 100 |
| Malaysia | 100 | 1 | 100 | 100 | 100 | 100 |
| Mexico | 100 | 1 | 100 | 100 | 100 | 100 |
| Moldova | 100 | 1 | 100 | 100 | 100 | 100 |
| Morocco | 100 | 1 | 100 | 100 | 100 | 100 |
| Netherlands | 100 | 1 | 100 | 100 | 100 | 100 |
| New Zealand | 100 | 1 | 100 | 100 | 100 | 100 |
| Nigeria | 100 | 1 | 100 | 100 | 100 | 100 |
| North Macedonia | 100 | 1 | 100 | 100 | 100 | 100 |
| Poland | 100 | 1 | 100 | 100 | 100 | 100 |
| Portugal | 100 | 1 | 100 | 100 | 100 | 100 |
| Romania | 100 | 1 | 100 | 100 | 100 | 100 |
| Russia | 100 | 1 | 100 | 100 | 100 | 100 |
| Saudi Arabia | 100 | 1 | 100 | 100 | 100 | 100 |
| Slovakia | 100 | 1 | 100 | 100 | 100 | 100 |
| Slovenia | 100 | 1 | 100 | 100 | 100 | 100 |
| Spain | 100 | 1 | 100 | 100 | 100 | 100 |
| Sweden | 100 | 1 | 100 | 100 | 100 | 100 |
| Switzerland | 100 | 1 | 100 | 100 | 100 | 100 |
| Taiwan | 100 | 1 | 100 | 100 | 100 | 100 |
| Tanzania | 100 | 1 | 100 | 100 | 100 | 100 |
| Thailand | 100 | 1 | 100 | 100 | 100 | 100 |
| Togo | 100 | 1 | 100 | 100 | 100 | 100 |
| Turkey | 100 | 1 | 100 | 100 | 100 | 100 |
| Uganda | 100 | 1 | 100 | 100 | 100 | 100 |
| United Arab Emirates | 100 | 1 | 100 | 100 | 100 | 100 |
| United States | 100 | 1 | 100 | 100 | 100 | 100 |

Figure 9 FR-CNN output(column detecting)

4.3 Conclusion from the model

This model further utilized recently published insights from deep learning-based semantic segmentation research for recognizing structures within tables. However, the model fails to resolve its persisting issues with recognizing structures which are in very close proximity to other elements of interest in an image. **Failure cases**

Hot topics by country

| Hot topics by country | Enquiries | Free movement of persons / workers | Enquiries |
|-----------------------|--------------|------------------------------------|--------------|
| Spain | 268 | Spain | 153 |
| Germany | 233 | Germany | 149 |
| United Kingdom | 139 | United Kingdom | 134 |
| France | 128 | France | 99 |
| Italy | 92 | Italy | 87 |
| Netherlands | 75 | Belgium | 49 |
| Austria | 66 | Netherlands | 48 |
| Portugal | 44 | Greece | 40 |
| Austria | 38 | Portugal | 34 |
| Finland | 35 | Ireland | 27 |
| Greece | 32 | Austria | 22 |
| Ireland | 34 | Sweden | 20 |
| Denmark | 32 | Ireland | 18 |
| Sweden | 33 | Denmark | 9 |
| Luxembourg | 9 | Luxembourg | 2 |
| Total EU-15 | 1,136 | Total EU-15 | 863 |
| Hungary | 17 | Bulgaria | 52 |
| Romania | 26 | Romania | 50 |
| Cyprus | 12 | Cyprus | 27 |
| Bulgaria | 9 | Poland | 20 |
| Czech Republic | 7 | Czech Republic | 13 |
| Estonia | 7 | Hungary | 11 |
| Poland | 7 | Latvia | 11 |
| Malta | 6 | Slovakia | 8 |
| Latvia | 3 | Lithuania | 7 |
| Slovakia | 3 | Estonia | 4 |
| Lithuania | 2 | Lithuania | 2 |
| Total EU-12 | 88 | Total EU-12 | 158 |
| non-EU | 97 | non-EU | 102 |
| Unspecified | 747 | Unspecified | 187 |
| Grand Total | 2,136 | Grand Total | 1,254 |

Figure 10 Close Columns

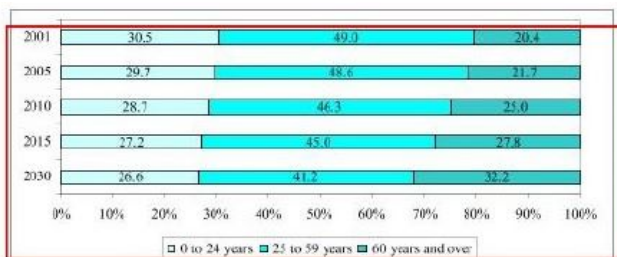


Figure 11 Bar chart confusion

| Sample Group | Some Year 1 Head Start Participation | No Year 1 Head Start Participation | Total |
|----------------------------------|--------------------------------------|------------------------------------|-------|
| All Randomly Assigned (N=4,667): | | | |
| 3-Year-Old Cohort | | | |
| Head Start Group | 85.1% | 14.9% | 100% |
| Control Group | 17.3% | 82.7% | 100% |
| 4-Year-Old Cohort | | | |
| Head Start Group | 79.8% | 20.2% | 100% |
| Control Group | 13.9% | 86.1% | 100% |

Figure 12 Nested row hierarchy

Table A-1. Summary of forecast assumptions to 2021

| Variable | Assumption |
|--|--|
| Demographic assumptions | |
| Population | Projections are consistent with the Census Bureau estimates. |
| 15- to 24-year-old population | Census Bureau projection: average annual growth rate of 0.1% |
| 25- to 29-year-old population | Census Bureau projection: average annual growth rate of 0.6% |
| 30- to 34-year-old population | Census Bureau projection: average annual growth rate of 1.3% |
| 35- to 44-year-old population | Census Bureau projection: average annual growth rate of 0.6% |
| Economic assumptions | |
| Disposable income per capita in constant dollars | Annual percent changes range between -1.9% and 2.2% with an annual growth rate of 1.4% |
| Education revenue receipts from state sources per capita in constant dollars | Annual percent changes range between -2.4% and 2.0% with an annual growth rate of 1.3% |
| Inflation rate | Inflation rate ranges between 1.0% and 2.0% |
| Unemployment rate (men) | |
| Ages 18 and 19 | Remains between 11.7% and 26.8% |
| Ages 20 to 24 | Remains between 10.8% and 15.6% |
| Age 25 and over | Remains between 5.3% and 7.9% |
| Unemployment rate (women) | |
| Ages 18 and 19 | Remains between 14.3% and 19.6% |
| Ages 20 to 24 | Remains between 9.3% and 13.1% |
| Age 25 and over | Remains between 5.0% and 7.3% |

*As the Census Bureau projections were not updated to reflect the 2011 Census Bureau population estimates, the Census Bureau age-specific

Figure 13 Very close rows

5 Model4:RCNN-HRNet

5.1 Pipeline architecture

It predicts the segmentation masks for tables of two types as bordered and borderless. Next in the pipeline, there are separate branches for bordered and borderless tables. Depending on the type of the detected table it is further processed by its respective branch post-processing module. Post-processing modules perform trivial tasks of arranging and cleaning the outputs of the model.

In the borderless branch, the predicted cells are detected inside the table are into rows and columns based on their positions. Then the model estimates the missing table lines using the positions of identified rows and columns. Based on these lines, for undetected cells, detect the cells using a contour-based text detection algorithm. And finally, Row-span and Col-span are also identified after estimating the lines.

In the bordered branch, a conventional algorithm of line detection is used to detect lines of bordered tables. The cells are identified using the line intersection points. And within each cell, the text regions are detected by using the contour-based text detection algorithm.

5.2 Algorithm

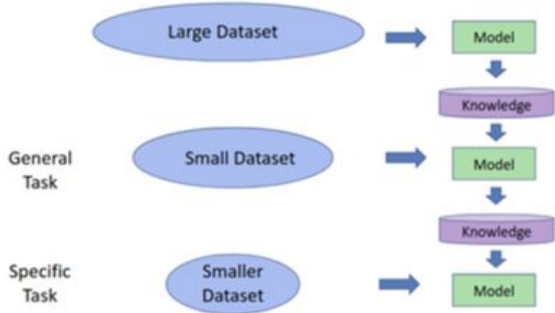


Figure 14 HRNet Algorithm

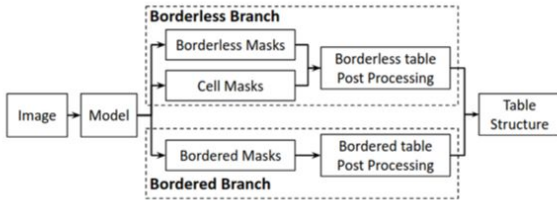


Figure 15 HRNet Pipeline

5.3 Conclusion from the model

The model starts learning for a general task and iteratively it learns to perform well on specific tasks. The model recognizes structures within tables by predicting table cell masks while using the line information as well. Improving the post-processing modules can further enhance the accuracy of the end-to-end model. The model performs better on various public datasets.

6 Experimental Analysis

Accuracy is a metric that generally describes how the model performs across all classes. It is useful when all classes are of equal importance. It is calculated as the ratio between the number of correct predictions to the total number of predictions.

Accuracy =

$$\frac{True_{positive} + True_{negative}}{True_{positive} + True_{negative} + False_{positive} + False_{negative}} \quad (1)$$

Precision is calculated as the ratio between the number of Positive samples correctly classified to the total number of samples classified as Positive (either correctly or incorrectly). The precision measures the model's accuracy in classifying a sample as positive.

$$Precision = \frac{True_{positive}}{True_{positive} + False_{positive}} \quad (2)$$

Recall is calculated as the ratio between the number of Positive samples correctly classified as Positive to the total number of Positive samples. The recall measures the model's ability to detect Positive samples. The higher the recall, the more positive samples detected.

$$Recall = \frac{True_{positive}}{True_{positive} + False_{negative}} \quad (3)$$

F1-score is a metric which takes into account both precision and recall

$$F1_{score} = 2 * \frac{Precision * Recall}{Precision + Recall} \quad (4)$$

| Model | Precision | Recall | F1 Score |
|------------------|-----------|--------|----------|
| R-CNN HRNet [1] | 0.9892 | 0.9921 | 0.9906 |
| Faster R-CNN [2] | 0.9615 | 0.9740 | 0.9677 |
| VGG-19 [3] | 0.9628 | 0.9697 | 0.9662 |
| YOLOv3 [4] | 0.9712 | 0.9821 | 0.9766 |

After thorough analysis of the metrics that affect the CNN models, we have come to the conclusion that the RCNN/HR-Net model has the best results for all the metrics. This model then proves to be the best among the other models presented in this report.

7 Conclusion

The report provides a detailed comparative analysis of table recognition. In the world of machine learning and deep learning, this topic is of great significance. Research in this domain has accelerated in recent years due to the growth of various deep-learning models, the complete method for identifying structures and detecting tables. It is demonstrated that current CNN architectures using instance segmentation, which were taught to recognise objects in photos of real scenes, are also highly good at detecting tables. Additionally, to learn well from a short quantity of data, picture augmentation methods and iterative transfer learning can be applied. The model begins by learning for a generic task, then over time, it progressively gains the ability to excel at more precise tasks. By predicting table cell masks while also employing line information, models -RCNN/HRNet, VGG-19, YOLOv3 and Faster-CNN can identify structures within tables. The accuracy of RCNN/HRNet is more than all the other models mentioned in the report. The accuracy of this model can be further improved by using post-processing modules. Our future work would be to further improve the HRNet model by training and testing it on other possible datasets and to overcome the present failure cases.

References

- [1] Prasad, D. et al. (2020) “Cascadetabnet: An approach for end to end table detection and structure recognition from image-based documents,” 2020 IEEE/CVF Conference on Computer Vision and Pattern Recognition Workshops (CVPRW) [Preprint]. Available at: <https://doi.org/10.1109/cvprw50498.2020.00294>.
- [2] Schreiber, S. et al. (2017) “DeepDeSRT: Deep Learning for detection and structure recognition of tables in document images,” 2017 14th IAPR International Conference on Document Analysis and Recognition (ICDAR) [Preprint]. Available at: <https://doi.org/10.1109/icdar.2017.192>.
- [3] Paliwal, S.S. et al. (2019) “TableNet: Deep Learning Model for end-to-end table detection and tabular data extraction from scanned document images,” 2019 International Conference on Document Analysis and Recognition (ICDAR) [Preprint]. Available at: <https://doi.org/10.1109/icdar.2019.00029>.
- [4] Huang, Y. et al. (2019) “A YOLO-based table detection method,” 2019 International Conference on Document Analysis and Recognition (ICDAR) [Preprint]. Available at: <https://doi.org/10.1109/icdar.2019.00135>.
- [5] S. Arif and F. Shafait. Table detection in document images using foreground and background features. In 2018 Digital Image Computing: Techniques and Applications (DICTA), pages 1–8, 2018.
- [6] Zhaowei Cai and Nuno Vasconcelos. Cascade r-cnn: Delving into high quality object detection. In The IEEE Conference on Computer Vision and Pattern Recognition (CVPR), June 2018.
- [7] Zhaowei Cai and Nuno Vasconcelos. Cascade R-CNN: high quality object detection and instance segmentation. CoRR, abs/1906.09756, 2019.
- [8] Kai Chen, Jiaqi Wang, Jiangmiao Pang, Yuhang Cao, Yu Xiong, Xiaoxiao Li, Shuyang Sun, Wansen Feng, Ziwei Liu, Jiarui Xu, Zheng Zhang, Dazhi Cheng, Chenchen Zhu, Tianheng Cheng, Qijie Zhao, Buyu Li, Xin Lu, Rui Zhu, Yue Wu, Jifeng Dai, Jingdong Wang, Jianping Shi, Wanli Ouyang, Chen Change Loy, and Dahua Lin. Mmdetection: Open mmlab detection toolbox and benchmark. CoRR, abs/1906.07155, 2019.
- [9] Zewen Chi, Heyan Huang, Heng-Da Xu, Houjin Yu, Wanxuan Yin, and Xian-Ling Mao. Complicated table structure recognition. ArXiv, abs/1908.04729, 2019.
- [10] J. Fang, X. Tao, Z. Tang, R. Qiu, and Y. Liu. Dataset, ground truth and performance metrics for table detection evaluation.
- [11] W. Farrukh, A. Foncubierta-Rodriguez, A. Ciubotaru, G. Jaume, C. Bejas, O. Goksel, and M. Gabrani. Interpreting data from scanned tables. In 2017 14th IAPR International Conference on Document Analysis and Recognition (ICDAR), volume 02, pages 5–6, 2017.
- [12] L. Gao, Y. Huang, H. D’ejean, J. Meunier, Q. Yan, Y. Fang, F. Kleber, and E. Lang. Icdar 2019 competition on table detection and recognition (ctdar). In 2019 International Conference on Document Analysis and Recognition (ICDAR), pages 1510–1515, 2019.
- [13] A. Gilani, S. R. Qasim, I. Malik, and F. Shafait. Table detection using deep learning. In 2017 14th IAPR International Conference on Document Analysis and Recognition (ICDAR), volume 01, pages 771–776, 2017.
- [14] Max Göbel, Tamir Hassan, Ermelinda Oro, and Giorgio Orsi. A methodology for evaluating algorithms for table understanding in pdf documents. In Proceedings of the 2012 ACM Symposium on Document Engineering, DocEng ’12, page 45–48, New York, NY, USA, 2012. Association for Computing Machinery.
- [15] M. Göbel, T. Hassan, E. Oro, and G. Orsi. Icdar 2013 table competition. In 2013 12th International Conference on Document Analysis and Recognition, pages 1449–1453, 2013.
- [16] D. He, S. Cohen, B. Price, D. Kifer, and C. L. Giles. Multiscale multi-task fcn for semantic page segmentation and table detection. In 2017 14th IAPR International Conference on Document Analysis and Recognition (ICDAR), volume 01, pages 254–261, 2017.